Geophysica (1987), Vol. 23, No. 2, pp. 113–141.
Printed in Finland

550.388

DEVELOPMENT OF THE AURORAL ELECTROJETS ON 16 MARCH 1978: AN EVENT STUDY

by

A. GRAFE (1), R.J. PELLINEN (2),
W. BAUMJOHANN (3), and M. VALLINKOSKI (2)

1) Heinrich-Hertz-Institut für Atmosphärenforschung und Geomagnetismus
der Akademie der Wissenschaften der DDR
DDR-1199 Berlin-Adlershof, Rudower Chaussee 5, GDR

2) Finnish Meteorological Institute,
Department of Geophysics
Box 503, SF–00101 Helsinki, Finland

3) Max-Planck-Institut für Physik und Astrophysik,
Institut für Extraterrestrische Physik,
D–8046 Garching, FR Germany

Abstract

Development of the convection eastward electrojet and the substorm westward electrojet is investigated for the time interval from 1730 to 1900 UT on 16 March 1978. For that purpose, observations of two Scandinavian and one Siberian magnetometer chain, the Scandinavian Twin Auroral Radar Experiment (STARE) and the all-sky camera at Kilpisjärvi are used. Different parameters of the electrojets are calculated and their relation to the electric field and the conductivity in this region are investigated. Following conclusions are made: (a) During the explosive phase, the eastward electrojet is wider than the westward one, though the current density and the total current have higher values in the westward electrojet. (b) The current density of the westward electrojet varies very much with latitude, while that of the eastward electrojet does not. (c) In the region of the eastward electrojet there is an anticorrelation between the northward component of the electric field and the ionospheric conductivity. (d) The centre of the eastward electrojet is located on the equatorward side of the conductivity and the northward electric field maxima. The electric field maximum is in the most poleward location.

1. *Introduction*

The existence of two auroral electrojets, the eastward electrojet in the evening sector, and the westward electrojet in the morning sector, is a well known fact. Most of the equivalent current systems derived from the bay-like variations of the geomagnetic field show more or less clearly the existence of these electrojets in the auroral zone (*e.g.*, VESTINE and CHAPMAN, 1938). At present, we know that the large-scale (global) convective eastward and westward electrojets are mainly driven by the magnetospheric electric field, which during quiet times maps down to the ionosphere. Also the ionospheric conductivities play an essential role, especially in disturbed conditions. During substorms, a substorm current wedge is superimposed on the convective westward electrojet in the midnight sector (*e.g.* PYTTE *et al.*, 1978, PELLINEN *et al.*, 1982). KAMIDE and VICKREY (1983) and KAMIDE and BAUMJOHANN (1985) identify two types of westward electrojet, a convection electrojet and a substorm electrojet. Enhanced precipitation in the latter case creates higher conductivity values and leads to a disturbed electric field pattern where also local polarisation fields extending over the highly conducting channel are important (*e.g.* BAUMJOHANN *et al.*, 1981).

A fundamental question raised in many studies dealing with auroral electrojets is the following one: How are the two electrojets coupled during disturbed conditions? Often this question has been answered by constructing tentative three-dimensional current systems. An extreme explanation was proposed by AKASOFU *et al.* (1965), who argued that the eastward electrojet in the evening sector is simply the return current of the westward electrojet. Numerous studies on the structure of the disturbed auroral electrojets made in the past using observations recorded by magnetometer chains have clearly shown that, in addition to the substorm current wedge, the eastward electrojet in the afternoon and evening sectors is an essential element of the magnetospheric substorm (see, *e.g.*, KISABETH and ROSTOKER, 1974, KAMIDE and AKASOFU, 1975, WALLIS *et al.*, 1976, TSUNODA *et al.*, 1976, MERSMANN *et al.*, 1979, BAUMJOHANN *et al.*, 1980, and USPENSKY *et al.*, 1983).

The large amount of particle energy which is transferred into the ionosphere during a substorm process enhances mainly the Hall conductivity at an altitude of about 100 km. This is most effective in the midnight and morning sectors, where the dynamics of the westward electrojet are determined to a large extent by the behaviour of the precipitating electrons (KAMIDE and BREKKE, 1977). On the contrary, particle precipitation does not play such an import role in the generation of the eastward electrojet (KAMIDE and VICKREY, 1983). More important in this region is probably the action of the strong poleward directed electric field (KAMIDE and BREKKE, 1977, KAMIDE and MATSUSHITA, 1979, ROSTOKER *et al.*, 1979, and

VICKREY *et al.*, 1982).

The transverse horizontal component of the electric field in the ionosphere is enhanced in the afternoon and evening sectors as shown by the observation of the Chatanika incoherent scatter radar (see, *e.g.*, HORWITZ *et al.*, 1978, and FOSTER *et al.*, 1982). The connection between the transverse electric field and the particle precipitation during the substorm process is, however, not clear at all. Often an anticorrelation is found between the electric field and the ionospheric conductivity especially in the region of the eastward electrojet (BAUMJOHANN *et al.*, 1980, VICKREY *et al.*, 1982, USPENSKY *et al.*, 1983).

In this paper the characteristic differences between the eastward and westward electrojets and the differences in their source mechanisms are studied. Also some common features in their development are searched. This is done by deriving some basic parameters of the auroral electrojets using magnetic ground-based data recorded on 16 March 1978.

2. *Observations and principles of data handling*

For the investigation of the large-scale structure of the eastward and westward electrojets of 16 March 1978, the following data were used:

(a) Magnetograms of profiles 2 and 4 of the Scandinavian Magnetometer Array (SMA, KÜPPERS *et al.*, 1979). The stations are listed in Table 1.
(b) Magnetograms of the magnetometer chain operated in Mid-Siberia as part of the Geomagnetic Meridian Project (see IMS Newsletter 8/1976). (Table 1).
(c) STARE data on the drift velocity of the ionospheric irregularities and the intensity of the backscattered radar signals from a region of 68°–72° geographic latitude and 15°–24° geographic longitude (see GREENWALD *et al.*, 1978).
(d) All-sky camera pictures recorded at Kilpisjärvi (69.0°N, 20.8°E).

One of the aims of this paper is to compare some parameters calculated for the eastward electrojet with the distribution and variations of the electric field and the ionospheric conductivity in the same region. Unfortunately, such a comparison can be done only in the northern part of profiles 2 and 4 of the SMA because of the limited coverage of STARE-observations in this region (see, *e.g.*, Fig. 1 in BAUMJOHANN *et al.*, 1980). From this point of view the comparison is rather incomplete. The STARE system gives information about the ionospheric electric fields and the ionospheric conductivities (GREENWALD, 1979, HALDOUPIS *et al.*, 1982). The irregularity drift velocity is approximately equal to the electron drift velocity, and can be used to estimate the ionospheric electric field. The backscatter amplitude

Table 1.

No. in Fig. 2	Symbol	Station	Geographic coordinates		Revised corrected geomagnetic coordinates (after GUSTAFSSON 1974)	
1	BEY	Beliy Island	73.3°N	70.0°E	67.8°N	146.0°E
2	TMB	Tambey	71.5	71.8	66.2	146.8
3	HAR	Harasvey	71.1	66.8	65.9	142.2
4	SEY	Seykha	70.1	72.5	65.1	146.2
5	CKA	Cape Kamenniy	68.5	73.6	63.6	146.4
6	AMD	Amderma	69.5	61.4	64.7	136.6
7	NDA	Nyda	66.6	73.0	61.8	145.9
8	UGU	Ugut	61.0	74.0	56.7	145.0
9	SOY	Söröya	70.6	22.2	67.4	107.9
10	MAT	Mattisdalen	69.9	22.9	66.6	107.8
11	MIE	Mieron	69.1	23.3	65.9	107.4
12	MUO	Muonio	68.3	23.6	64.8	106.7
13	PEL	Pello	66.9	24.7	63.5	106.6
14	OUL	Oulu	65.1	25.5	61.8	106.1
15	SAU	Sauvamäki	62.3	26.7	58.8	105.3
16	AND	Andenes	69.3	16.0	66.6	102.4
17	EVE	Evenes	68.5	16.8	65.8	102.2
18	RIJ	Ritsemjokk	67.7	17.5	64.9	102.1
19	KVI	Kvikkjokk	66.9	17.9	64.1	101.7
20	SRV	Storavann	65.8	18.2	62.9	101.0
21	LYC	Lycksele	64.6	18.7	61.7	100.6

is related to the mean (ambient) electron density, and can therefore be used to estimate the Hall conductivity. In studying this same event, USPENSKY *et al.*, (1983) found a linear relationship between the STARE backscatter amplitude and the Hall conductivity.

In this work, we use uncorrected STARE intensity data, which is sufficient due to the following reasons. First of all, only intensities recorded by the Finnish radar, looking more or less perpendicular to the electron flow, are used. Hence, flow angle corrections are unimportant. Secondly, the aspect angle and range corrections are small within the region of the eastward electrojet, located in the lower part of the STARE field of view. Finally, we are interested only in two features: the location of the conductivity maximum in the eastjet and the temporal variations of the conductivity at a specified point.

The magnetograms from the three different meridional chains were used to calculate the following parameters:

1) Position of the centre of the electrojet;

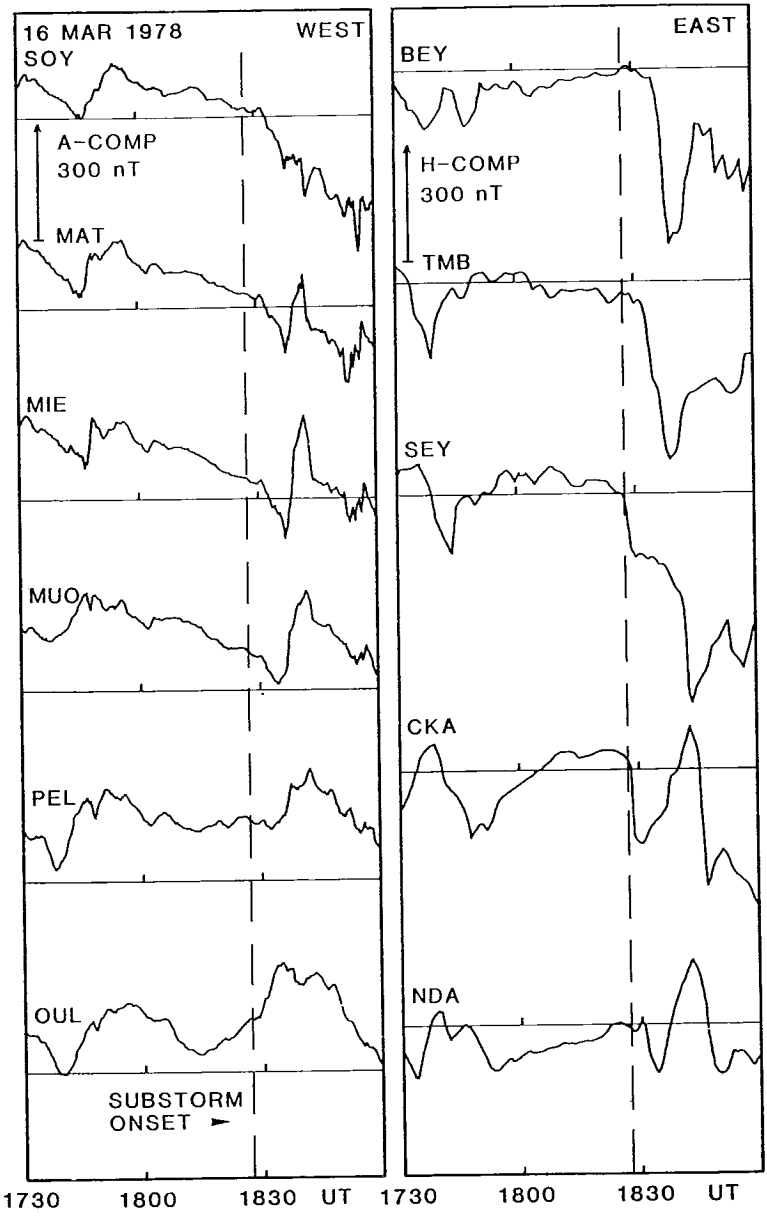

Fig. 1. A-components of Profile 4 of the Scandinavian Magnetometer Array (left panel) and H-components of the Mid-Siberian magnetometer chain (right panel) for the substorm event on 16 March 1978.

2) Width of the current sheet, which was assumed to be infinitely thin at a height of 120 km;
3) The height-integrated current density;
4) The total current intensity;
5) The direction of the equivalent current vector with respect to the revised corrected geomagnetic north.

The centre of the electrojet was defined as usual by the zero cross-over of the magnetic vertical disturbance field along a latitudinal profile. Whenever necessary, current-sheet width, current density and total current intensity were calculated separately for the two regions poleward and equatorward of the electrojet center. In general, the current density of the electrojets changes along the meridian. To simplify matters, we assumed in our calculations a constant current density over the whole electrojet width. This does not resemble the real situation, but as GRAFE (1978) has shown the calculated values for width and total current intensity are almost independent of the form of the current density profile. The same is valid for the current density averaged over the profile. Therefore, this assumption of a uniform current density gives a mean for the current density. The calculation of the electrojet parameters was performed with the method described by GRAFE (1978); for details see Appendix 1.

Model curves of the ratio $\Delta H/\Delta Z$ along a profile perpendicular to the current sheet for different values of current-sheet width were calculated according to the general relations of the magnetic horizontal and vertical components of a current sheet, as given, *e.g.*, by CHAPMAN (1951). The width of the current sheet was obtained by comparing the observed latitudinal profiles of the $\Delta H/\Delta Z$ ratio with those model curves. It could be shown that induction effects have no essential importance for the typical variations in the electrojets (see also KÜPPERS *et al.*, 1979). The estimation of the width of the electrojet has an accuracy of about ± 40 km. The accuracy in the current density and in the total current intensity lies within $\pm 15\,\%$. These values result from the error in the calculation of the disturbance vector and from the error in the graphical method in the comparison between observational and model curves.

In calculating the parameters, not the whole horizontal magnetic disturbance vector was used, but only the part caused by the »real ionospheric electrojet current». This »real electrojet current» was obtained assuming the electrojets flow in the revised corrected geomagnetic east-west direction and are infinitely extended in longitude. Thus the electrojet current could be related to the magnetic perturbations in the revised corrected geomagnetic north-south direction.

3. *Results of the data analysis*

a) General character of the disturbances

On the evening of 16 March 1978 at 1827 UT, a substorm onset occurred to the east of Scandinavia. The break-up was preceded by a relatively quiet period, resembling an interval between two moderate substorms. During this period, some growth phase features were observed, as described in detail in USPENSKY *et al.*, (1983).

The variations in the SMA magnetic field (profile 4, *A* component) and in the Mid-Siberian profile (*H* component) are shown in Fig. 1. Between 1730 to 1830 UT, all stations display pronounced disturbances. After 1800 UT the positive disturbances in SMA decrease while a minor substorm over Siberia is recovering. Later the positive disturbances intensify in the west at the southernmost stations. Poleward to this region strong negative disturbances appear. The positive disturbances last until about 1900 UT.

In Fig. 1 we also see that between 1800 to 1830 UT the Mid-Siberian magnetometer chain is obviously situated within the Harang discontinuity region. After 1830 UT, strong negative bay disturbances appear at all stations in this region. Especially the time interval from 1830 to 1900 UT is suitable for investigating the influences of substorm activity on the development of westward and eastward electrojets. However, to study some special features of the eastward electrojet in more detail, the whole time interval from 1730 to 1900 UT has to be analysed.

Fig. 2 shows the equivalent current vectors in the Scandinavian and Mid-Siberian regions at three different instants. At 1806 UT, a substorm growth phase was in progress and a pronounced rather broad eastward electrojet existed in the Scandinavian region. The Mid-Siberian magnetometer chain shows latitudinal variation in the directions of the current vectors, a feature typical of the Harang discontinuity (see, *e.g.*, HARANG, 1946, HEPPNER, 1972, KAMIDE, 1978). At 1838 UT, a clear westward electrojet associated with the substorm is flowing in the Mid-Siberian region. This substorm-related westward electrojet is observed to flow to the north of the eastward electrojet in the Scandinavian sector. At 1854 UT a pronounced eastward electrojet is observed over Scandinavia and a broad westward electrojet over Mid-Siberia. Under these circumstances, calculation of the parameters for the eastward electrojet for the whole time interval from 1730 to 1900 UT and for the westward electrojet for the time interval from 1830 to 1900 UT is possible.

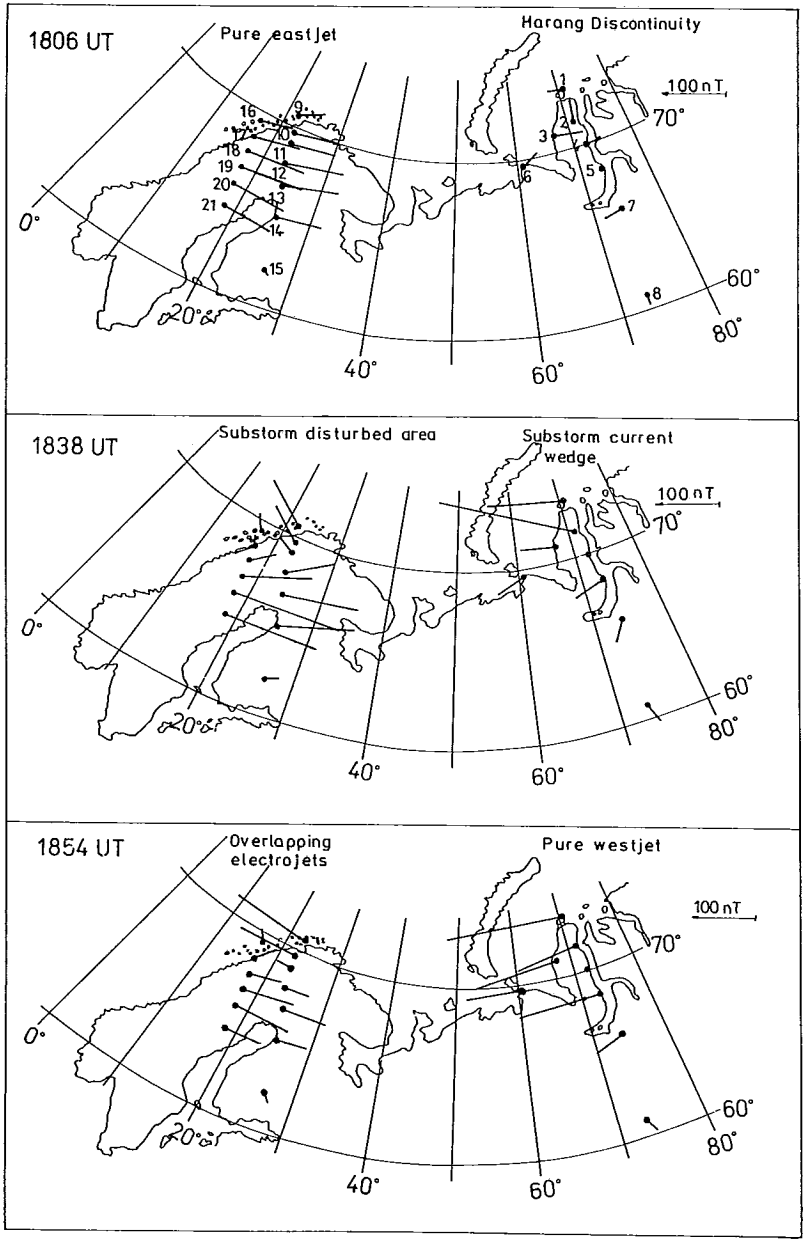

Fig. 2. Equivalent current vectors in the Scandinavian and Mid-Siberian regions at three different instants. The numbers of the stations refer to Table 1.

b) Variations in the electrojet parameters

The parameter values for each 2 minutes of the electrojets were determined according to the method explained in Section 2. Fig. 3 shows curves for the different parameters of the eastward electrojet calculated for profile 2 of the SMA. Figs. 4a and 4b show the parameter-time diagrams for profile 4 of the SMA and for the Mid-Siberian profile. These diagrams characterize mainly the large-scale variations of the two electrojets, since the short-period changes have been more or less eliminated. Negative values in height-integrated current density and total current are related to the westward and positive values to the eastward current. After the substorm onset, the centre of the westward electrojet in the Mid-Siberian sector shifts suddenly 4 degrees polewards while the location of the eastward electrojet centre stays almost constant.

Table 2 summarizes the time-averaged values of the parameters. The mean width of both electrojets attains a value of about 500 km. For the time interval from 1830 to 1900 UT, for which a direct comparison between the two electrojets

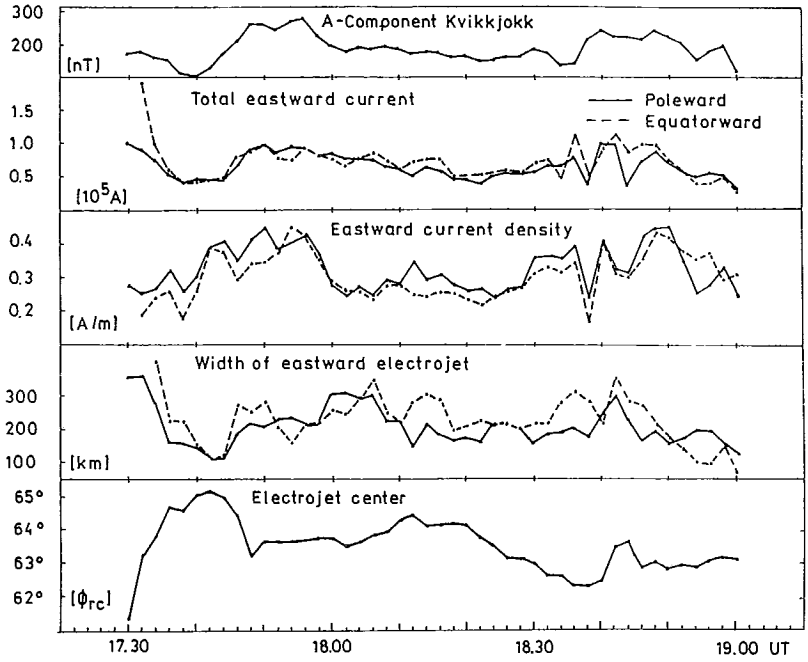

Fig. 3. Parameter-time diagram for the eastward electrojet (1730–1800 UT on 16 March 1978). The parameters were calculated by using the magnetograms of Profile 2.

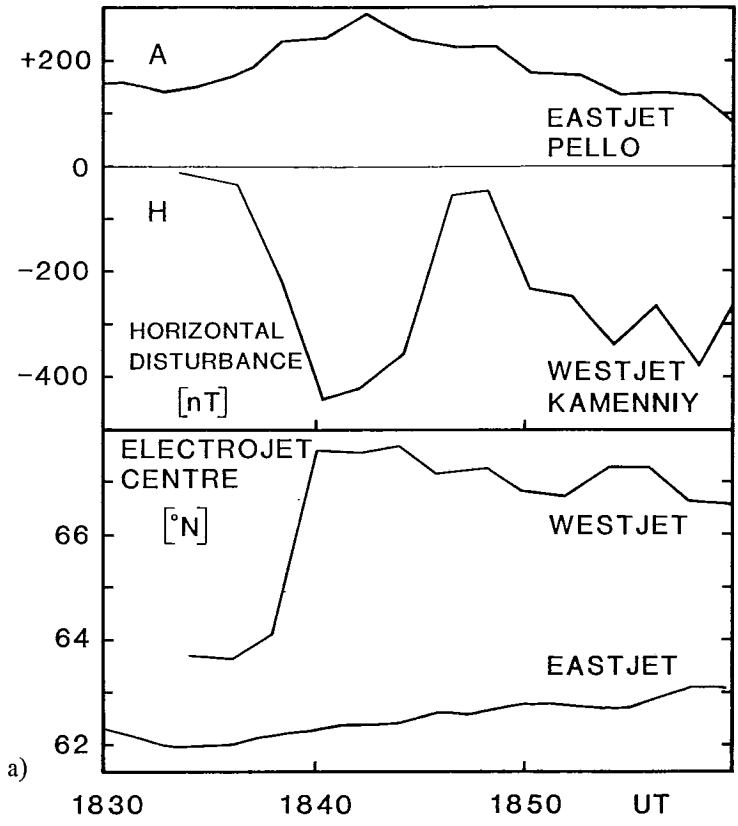

Fig. 4a, b. Same as Fig. 3, but for 1830 to 1900 UT and for both electrojets. The parameters for the eastward electrojet were calculated from Profile 2 and those for the westward electrojet from the magnetograms of the Mid-Siberian profile.

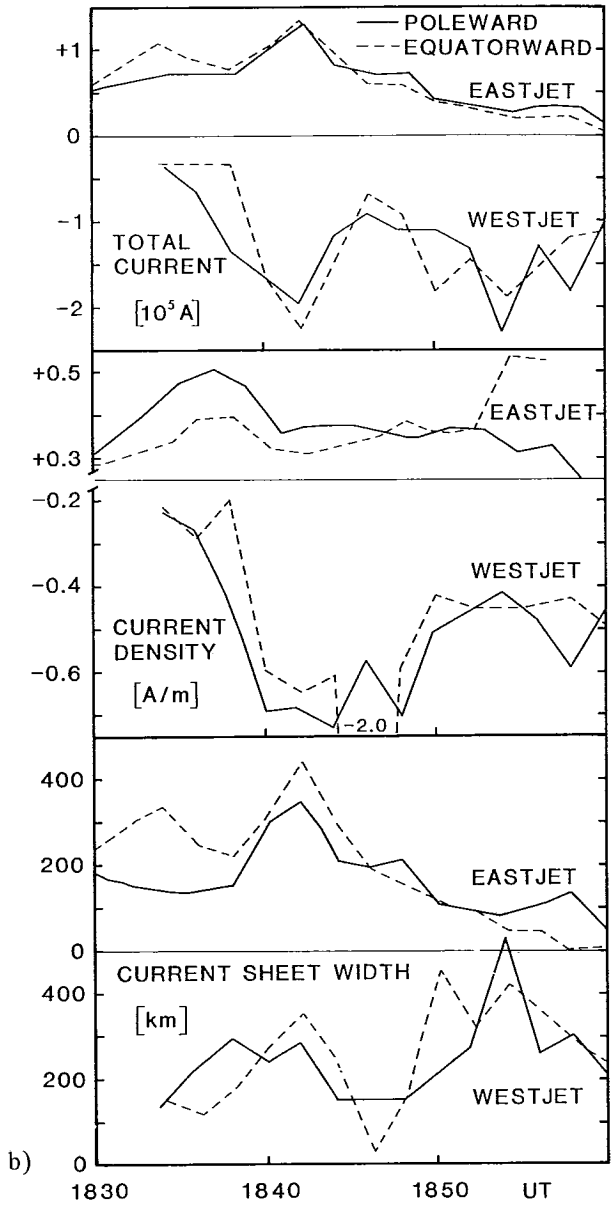
POLEWARD
EQUATORWARD
+1
0
EASTJET
-1
-2
TOTAL
CURRENT
[10⁵A]
WESTJET
+0.5
+0.3
EASTJET
-0.2
-0.4
-0.6
CURRENT
DENSITY
[A/m]
WESTJET
-2.0
400
200
0
EASTJET
CURRENT SHEET WIDTH
400
200
0
[km]
WESTJET
1830
1840
1850
UT

b)

Fig. 4b.

Table 2. Time-averaged parameter values.

	Scandinavian region				Mid-Siberian region
	1730–1830 UT		1830–1900 UT		1830–1900 UT
	Profile 2	Profile 4	Profile 2	Profile 4	
Electrojet width (km)					
equatorward	286	255	210	206	255
poleward	226	216	190	167	250
Height-integrated current density (mA m^{-1})					
equatorward	290	260	340	370	550
poleward	320	290	340	350	520
Total current (kA)					
equatorward	156	134	67	63	121
poleward	142	125	64	59	127

is possible, the main results are the following:

1. The time-averaged value of the width of the substorm enhanced westward electrojet is slightly greater than that of the eastward electrojet. However, during the substorm explosion phase (1843 UT) the eastward electrojet is wider than the westward electrojet.
2. The current density in the substorm enhanced westward electrojet is greater than in the eastward electrojet.
3. The total current intensity of the substorm enhanced westward electrojet is two times higher than that of the eastward electrojet.
4. The differences in the parameter mean values calculated separately for the poleward and equatorward parts of the electrojets are small.

A careful investigation of the parameter-time diagrams reveals that during some large variations in the electrojet width, changes in the current density as well as in the total current intensity are more pronounced in the westward than in the eastward electrojet. In Figs. 5 and 6 we show the dependence of the current density and the total current intensity on the electrojet width, respectively. Fig. 6 presents a comparison between westward and eastward electrojets and the results can be summarized as follows:

1. The scatter of the data points is smaller in the eastward electrojet than in the westward electrojet, as seen in the relationships between the current density and the width (upper panel) and between the total current and the width

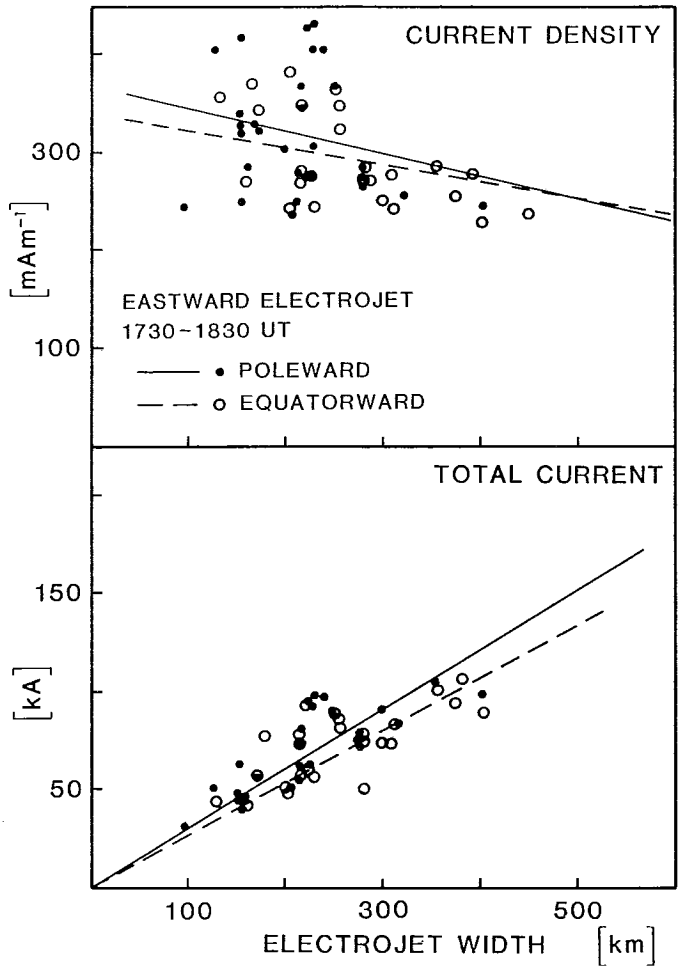

Fig. 5. Relationship between current density and electrojet width and between total current intensity and electrojet width for the eastward electrojet during the growth phase (1730–1830 UT). The straight lines refer to a linear regression.

(lower panel). In Table 3 the scatter is given in absolute values. However, for example, the current density of the westward electrojet (Table 2) is not even two times greater than the current density of the eastward electrojet whereas the scatter is nearly one and a half order of magnitude greater.

2. The variations in the current density in the westward electrojet are greater than in the eastward electrojet.

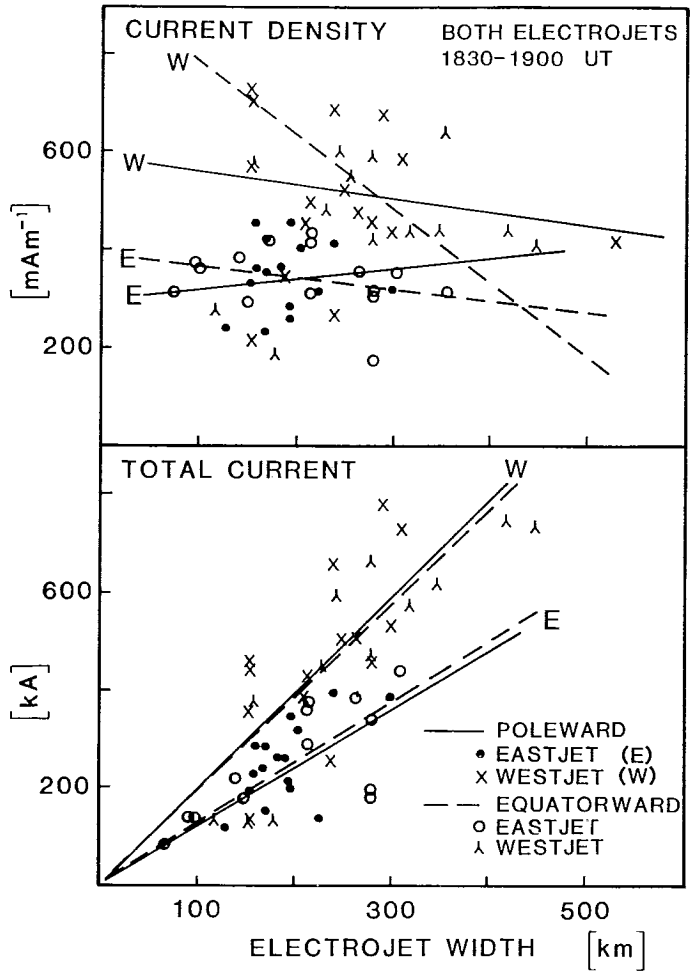

Fig. 6. Same as in Fig. 5, but for both eastward and westward electrojets during the substorm expansion phase (1830–1900 UT).

3. The increase in total current intensity during the expansion of the electrojet width is stronger in the westward electrojet than in the eastward electrojet.

The averaged values of the parameters are summarized in Table 3. They show the same trends as reported above. Especially striking is the greater variance in the current density and the total current for the westward electrojet. An informative value obtained from Figs. 5 and 6 is the relative change of the current density and of the total current intensity for a change of 100 km in the width. Also these

Table 3. Variance and relationships between the parameters.

	Scandinavian region (eastward electrojet)				Mid-Siberian region (westward electrojet)
	1730–1830 UT		1830–1900 UT		1830–1900 UT
	Profile 2	Profile 4	Profile 2	Profile 4	
Variance (σ_i^2) in current density (A^2m^{-2})					
equatorward	$3.38\ 10^{-3}$	$1.10\ 10^{-3}$	$3.64\ 10^{-3}$	$5.57\ 10^{-3}$	$1.79\ 10^{-1}$
poleward	$3.26\ 10^{-3}$	$2.65\ 10^{-3}$	$4.58\ 10^{-3}$	$4.81\ 10^{-3}$	$3.18\ 10^{-1}$
Variance (σ_I^2) in total current (A^2)					
equatorward	$4.02\ 10^{9}$	$2.14\ 10^{9}$	$7.13\ 10^{8}$	$1.21\ 10^{9}$	$5.08\ 10^{10}$
poleward	$1.82\ 10^{9}$	$1.15\ 10^{9}$	$3.96\ 10^{8}$	$8.04\ 10^{8}$	$3.48\ 10^{10}$
Differential change in current density (di/dc) related to changing width ($\cdot 10^{-3}\,Am^{-2}$)					
equatorward	$-0.16\ 10^{-3}$	$0.14\ 10^{-3}$	$-0.22\ 10^{-3}$	$-0.51\ 10^{-3}$	$-1.54\ 10^{-3}$
poleward	$-0.24\ 10^{-3}$	$-0.17\ 10^{-3}$	$0.16\ 10^{-3}$	$0.14\ 10^{-3}$	$-0.27\ 10^{-3}$
Differential change in total current (dI/dc) related to changing width ($\cdot 10^{-3} Am^{-1}$)					
equatorward	272	270	310	329	468
poleward	300	290	333	355	494
Relative change ($\Delta i/i$) in current density (%)					
equatorward	-5.5	5.4	-6.5	-13.8	-28.1
poleward	-7.4	-5.5	4.7	4.1	-5.2
Relative change ($\Delta I/I$) in total current (%)					
equatorward	30.8	39.8	46.3	52.2	38.7
poleward	43.0	47.0	52.0	60.2	38.9

values are given in Table 3. From these values it can be concluded that the relative changes in the current intensities of both electrojets are far greater than the relative changes of the current densities. This is not surprising because the total current intensity is equal to the product of the electrojet width and of the current density. In this context, a comparison between the eastward and westward electrojets for the time interval from 1830 to 1900 UT shows clearly that also the relative changes in the current density of the eastward electrojet are smaller than those of the west-

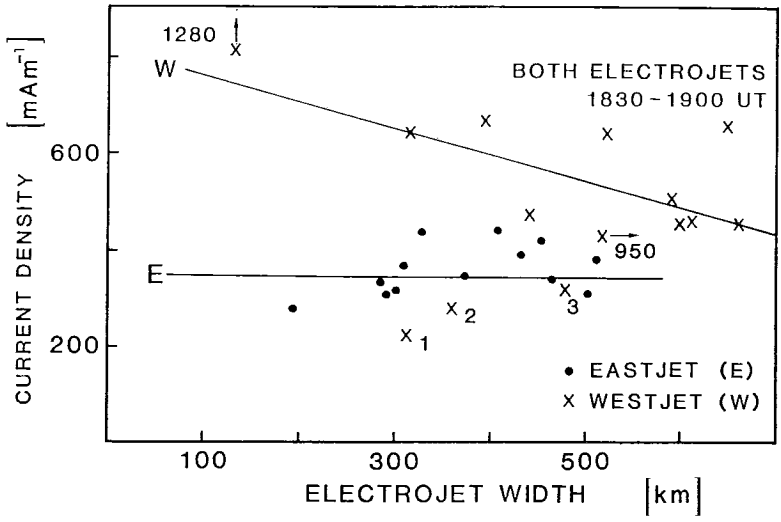

Fig. 7. Relationship between current density and current sheet width of the two electrojets during the expansion phase (1830–1900 UT).

ward electrojet. However, the relative changes of the total current intensity are greater. Again, the absolute changes of the total current intensity of the eastward electrojet are smaller than those for the westward electrojet, but the relative changes are greater.

The values in Table 3 show still another fact. The current density of the poleward part as well as of the equatorward part of the westward electrojet decreases with increasing electrojet width. On the other hand, in the region of the eastward electrojet the current density in the equatorward part increases slightly with enhancing width and decreases in the poleward part. Fig. 7 shows the dependence of the current density on the width by using values averaged over the poleward and equatorward halves. This result is unambiguous and confirms the opinion presented already by LOGINOV *et al.*, (1978) that the current density of the eastward electrojet is influenced only a little by changes in the width. It should be taken into account that the crosses in Fig. 7 designated by 1, 2 and 3 are points before the active substorm phase when the electrojet is not well developed. Therefore, these points are not significant.

c) Variations in the parameters observed by STARE

Due to the limited spatial coverage of the STARE observing area, we have no radar observations from the region of the westward electrojet, and only a limited

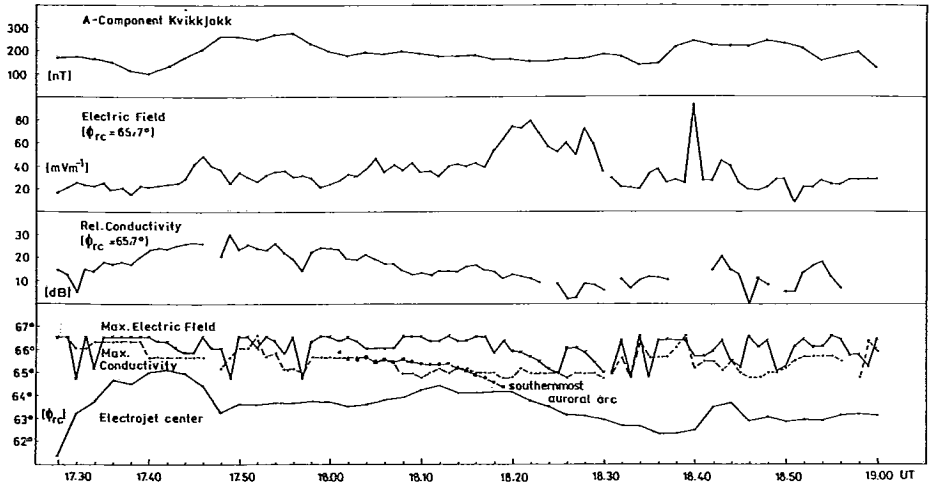

Fig. 8. Parameter-time diagram of the position (in revised corrected latitude ϕ_{rc}) of the electrojet center, of the conductivity maximum (backscatter max), electric field maximum and southernmost auroral arc (bottom panel), of the logarithm of the conductivity (the SNR of the Finnish radar in dB) and the electric field for ϕ_{rc} = 65.7°N (two middle panels) and of the A-component of Kvikkjokk (top panel).

area of the eastward electrojet is covered.

In the bottom panel of Fig. 8 (profile 2) the latitudinal changes in four different parameters are shown: the position of the electrojet centre, the location of the observed conductivity maximum, maximum of the observed electric field and the location of the southernmost auroral arc observed at Kilpisjärvi before 1830 UT. ϕ_{rc} is the revised corrected geomagnetic latitude (GUSTAFSSON, 1974). From these curves we see the following:

1. In the eastward electrojet, the electric field maximum occurs poleward of the conductivity maximum.
2. The centre of the eastward electrojet is located equatorward of the electric field maximum and probably also equatorward of the conductivity maximum.

The latter can be concluded also from the magnetic ground-based data alone. Fig. 9 clearly shows that the current density is greater on the poleward side of the electrojet center. By comparing the behaviour of the poleward and equatorward parts of the two electrojets during the time from 1830 to 1900 UT (Fig. 10), it seems that the current density is greater poleward than equatorward of the

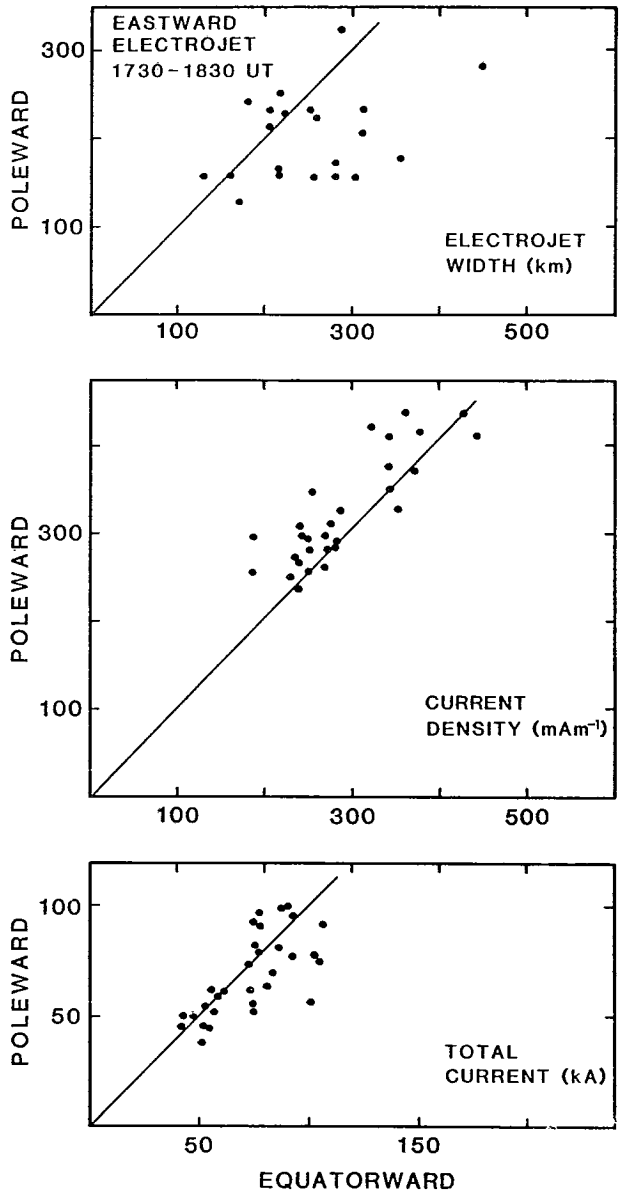

Fig. 9. Comparison of the electrojet parameters of the poleward (vertical axis) and equatorward (horizontal axis) halves for the eastward electrojet between 1730 and 1830 UT. The diagonals in each frame refer to the poleward = equatorward line.

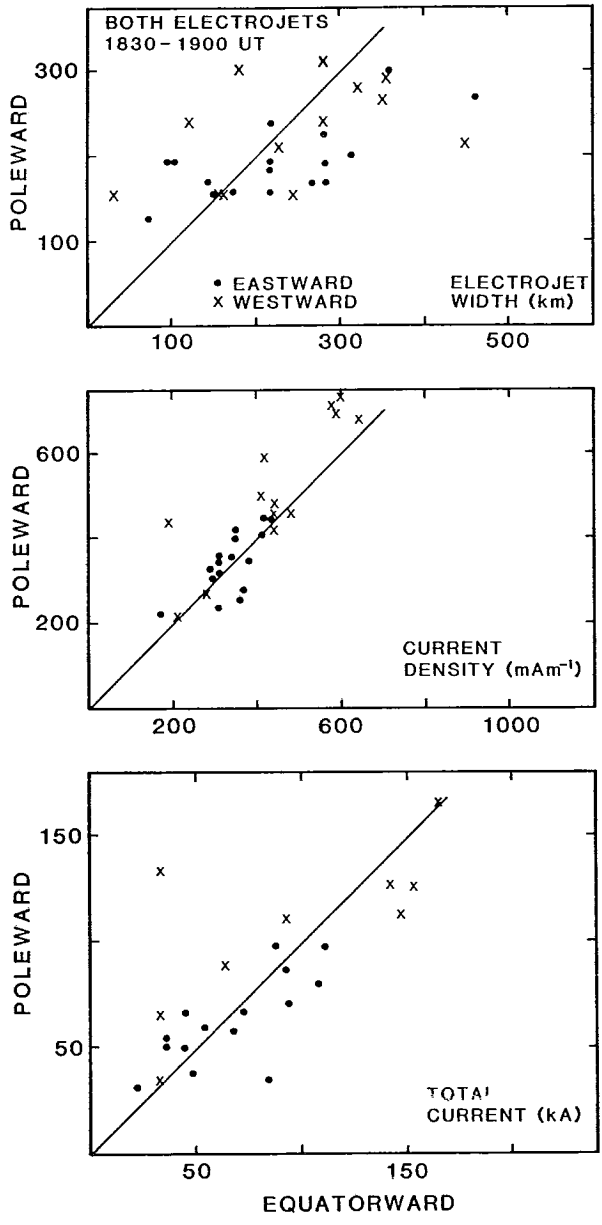

Fig. 10. Same as in Fig. 9, but for both eastward and westward electrojets between 1830 and 1900 UT.

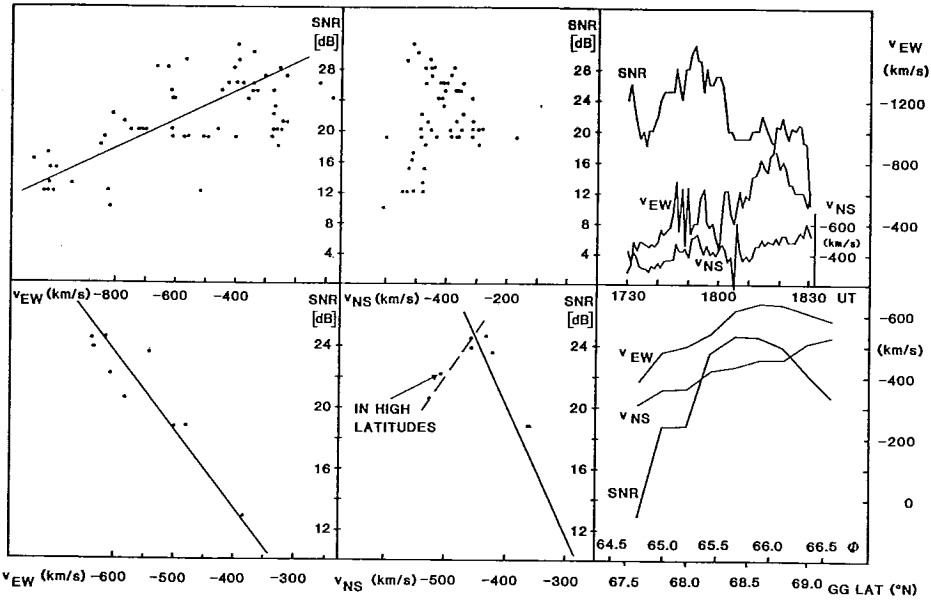

Fig. 11. Upper part: Profile-averaged values of the drift velocity components V_{EW} (corr. geom. EW) and V_{NS} (corr. geom. NS) and of the backscatter signal intensity. Lower part: Time-averaged values of the same parameters as for the upper part.

center for both electrojets. On the other hand, the picture is not as clear for the relationships between the poleward and equatorward widths and total currents. It must be emphasized that in the equatorward part of the eastward electrojet, the current density increases slightly with increasing width while poleward of the center, it decreases slightly. This is not the case for the westward electrojet as clearly shown in Fig. 6 and Table 3.

Similar differences in the position of the electric field maximum and the conductivity maximum in the afternoon sector have been reported in USPENSKY *et al.*, (1983).

The two middle panels in Fig. 8 show the variations in the electric field and the logarithm of the conductivity (the uncorrected SNR of Finnish radar) over one station of profile 2.

In Fig. 11, for the period from 1730 to 1830 UT, the values of the logarithm of the conductivity averaged over profile 2 and the components of the drift velocity are represented in corrected geomagnetic coordinates in the upper part, in the lower part are the values averaged over the period from 1730 to 1830 UT along profile 2.

1. In the period from 1730 to 1830 UT the westward directed electric field (= V_{NS}) rarely varies, but the northward directed (= V_{EW}) does.
2. With the beginning of intensification of the eastward electrojet from approx. 1750 UT (see Fig. 1), a distinct anticorrelation between the conductivity and the northward directed electric field can be noticed.
3. The time-averaged values of the conductivity and the electric field show a characteristic latitudinal profile where the conductivity maximum occurs somewhat more to the south than the maximum of the northward electric field. The centre of the eastward electrojet is about 2 degrees more southward (see also Fig. 8 for the instantaneous values).
4. There is a good correlation between the conductivity and the northward component of the electric field along the profile.

4. *Discussion*

In this investigation the analysis of the geomagnetic data from meridional chains is carried out in such a way that only the large-scale structures of auroral electrojets are considered. It is not unambiguously clear if in the case of negative horizontal magnetic disturbances we have to suppose effects of a DP1 or a DP2 current system in the differentiation between the two different westward electrojets as suggested by KAMIDE (1982).

Though it is well known that during magnetospheric disturbances, the eastward electrojet reaches a lower activity level than the westward one, the physical nature of the eastward electrojet and its generation mechanism are by no means completely explained. Is it an element of the large-scale convection process or is it activated by other elements of the substorm process, too? BAUMJOHANN *et al.*, (1980) introduced the concept of »substorm-intensified eastward electrojet». The investigations presented in this work, however, also are unable to give the desired answer to this question, in particular because only one event is investigated, which means that the results cannot be generalized.

The analysis of the observational material, however, yields results which are of importance in regard to the different structure of both electrojets and to the eastward electrojet in its relation to conductivity and electric field. These results are summarized as follows:

1. During the explosion phase the eastward electrojet is wider than the westward one, though the current density and the total current intensity of the westward electrojet reach higher values.
2. The variations of the current density in the westward electrojet are greater than those in the eastward one. The current density increases in the westward electro-

jet along with the width while it hardly varies in the eastward electrojet.

3. In the eastward electrojet the northward and westward components the electric field vary only slightly. A pronounced anticorrelation exists between the northward component of the electric field and the ionospheric conductivity.
4. The centre of the eastward electrojet is located on the equatorward side of the conductivity and the northward electric field maxima. The electric field maximum is in the most poleward location.

The first result shows distinct differences between the eastward and the westward electrojets. Although the energy brought into the ionosphere is higher in the region of the westward electrojet, the area of energy injection into the ionosphere is obviously greater in the eastward electrojet. This result is typical for the explosion phase in this event and thus the concept of DP1-type substorm westward electrojet around midnight cannot be extended to the convection westward electrojet in the morning sector. The reason in this case might be that the eastward electrojet, as shown by KAMIDE and VICKREY (1983), is produced mainly by the large-scale electric field than by particle precipitation. The particle precipitation producing the substorm-related westward electrojet is obviously confined to a restricted area.

Figs. 9 and 10 distinctly show that the current density is greater for both electrojets in the poleward part of the electrojet (see also USPENSKY *et al.*, 1983). Hence, for both electrojets a model of asymmetric current density distribution with geomagnetic latitude is applicable. Naturally, this emphasizes the significance of particle precipitation for the generation of both electrojets. However, still another indication, to be discussed in the last paragraph, has been found which points to the influence of particle precipitation in the generation of the eastward electrojet.

An essential result of this paper is the relation of electrojet current density to the electrojet width. This relationship is different for the two electrojets as shown in Fig. 6 and Table 3. These differences are most distinct if the parameters are calculated for the entire electrojet as shown in Fig. 7. The question to be raised is: Why does the current density of the eastward electrojet vary so little with width while the current density of the westward electrojet varies greatly? In fact, we may conclude that in the eastward electrojet there is an anticorrelation between the transverse electric field and the conductivity. This is distinctly shown in Fig. 11. Since the height-integrated current density is the product of the height-integrated conductivity and the horizontal electric field, an anticorrelation of conductivity and electric field can lead to approximately constant values of current density.

Fig. 7 as well as Table 3 show that the current density in the westward electrojet is higher than in the eastward electrojet. Hence, the broadening of the electrojet is connected with a faster increase in the total current of the westward electrojet than in the eastward electrojet. This means that the enhancement of the energy input from the plasma sheet during the expansion of the precipitation region must be higher in the region of the westward electrojet than in the region of the eastward electrojet.

In order to understand the development of the eastward electrojet during substorms, the physical process governing the observed relationship between the electric field and the conductivity has to be known, which is not the state of the art at the moment. As we have observed, the electric field maximum occurs somewhat poleward of the conductivity maximum. This means that in the plasma sheet, particles are accelerated in an area closer to the Earth than the region where the electric field reaches its maximum values.

Characteristic differences between the eastward and westward electrojets have also been found by CLAUER *et al.*, (1981). They found that the AL activity (activity of the westward electrojet) depends very much on the solar wind parameters, but the AU activity (activity of the eastward electrojet) does not show a clear dependence on the solar parameters. Similar results were obtained by SPRENGER and GRAFE (1984), who investigated the dependence of the occurrence of radar auroras on the sector structure of the IMF and found that radar auroras occurring in the evening sector do not depend on the sector structure, but the radar auroras in the morning sector show a considerable dependence on the sector structure. These results are in good agreement with the above mentioned ones. There, however, still remains the question about the process causing the anticorrelation between the electric field and the conductivity. Or are there in the case of the eastward electrojet two different generation mechanisms, too, where one is determined by the electric field and the other one by the effect of particle precipitation? In order to answer these questions further investigations have to be done.

Acknowledgements. The STARE data were provided by the Max-Planck-Institute für Aeronomie and the Mid-Siberian magnetometer data by the IZMIRAN in Moscow. The USSR magnetic data were digitized and replotted at the Sodankylä Geophysical Observatory. We are grateful to these institutes and to the persons responsible for the actions. The SMA observations and the work of W.B. were financially supported by grants from the Deutsche Forschungsgemeinschaft. The cooperation between three of us (A.G., R.P. and M.V.) was financially supported by the Academy of Finland and the Academy of Sciences of GDR.

REFERENCES

AKASOFU, S.I., CHAPMAN, S. and C.I. MENG, 1965: The polar electrojet. *J. Atmos. Terr. Phys.* **27**, 1275–1305.

BAUMJOHANN, W., UNTIEDT, J. and R.A. GREENWALD, 1980: Joint two-dimensional observations of ground magnetic and ionospheric electric fields associated with auroral zone currents. 1. Three-dimensional current flows associated with a substorm – intensified eastward electrojet. *J. Geophys. Res.* **85**, 1963–1978.

BAUMJOHANN, W., PELLINEN, R.J., OPGENOORTH, H.J. and E. NIELSEN, 1981: Joint two-dimensional observations of ground magnetic fields associated with auroral zone currents: current systems associated with local auroral break-ups. *Planet. Space Sci.* **29**, 431–447.

CHAPMAN, S., 1951: The equatorial electrojet as detected from the abnormal electric current distribution above Huancayo, Peru and elsewhere. *Arch. Meteorologie, Geophys., Bioklimatol. Serie A, Bd. IV* 368–390.

CLAUER, C.R., McPHERRON, R.L., SEARLS, C., and M.G. KIVELSON, 1981: Solar wind control of auroral zone geomagnetic activity. *Geophys. Res. Lett.* **8**, 915–918.

FOSTER, J.C., BANKS, P.M. and J.R. DOUPNIK, 1982: Electrostatic potential in the auroral ionosphere derived from Chatanika radar observations. *J. Geophys. Res.* **87**, 7513–7524.

GRAFE, A., 1978: Die auroralen Elektrojets. *HHI-STP-Report 11.*

GREENWALD, R.A., 1979: Studies of currents and electric fields in the auroral zone ionosphere using radar auroral back-scatter, in *Dynamics of the magnetosphere,* edited by S.-J. Akasofu, pp. 213–248, D. Reidel, Dordrecht.

GREENWALD, R.A., WEISS, W. and E. NIELSEN, 1978: STARE: A new radar auroral backscatter experiment in northern Scandinavia. *Radio Science,* **13**, 1021–1039.

GUSTAFSSON, G., 1974: A revised corrected geomagnetic coordinate system. *Arkiv for Geofysik,* **5**, 595–617.

HALDOUPIS, C., NIELSEN, E. and C.K. GOERTZ, 1982: Experimental evidence on the dependence of 140-Magahertz radar auroral backscatter characteristics on ionospheric conductivity. *J. Geophys. Res.* **87**, 7666–7670.

HARANG, L., 1946: The mean field of disturbance of polar geomagnetic storms. *Terr. Magn.* **51**, 353–380.

HEPPNER, J.P., 1972: The Harang discontinuity in auroral belt ionospheric currents. *Geofys. Publ.* **29**, 105–120.

HORWITZ, J.L., DOUPNIK, J.R. and P.M. BANKS, 1978: Chatanika radar observations of the latitudinal distributions of auroral zone electric fields, conductivities and currents. *J. Geophys. Res.* **83**, 1463–1481.

IMS Newsletter **8**, 6, 1976.

KAMIDE, Y., 1978: On current continuity at the Harang discontinuity. *Planet. Space Sci.* **26**, 237–244.

–»– , 1982: The two-component auroral electrojet. *Geophys. Res. Lett.* **9**, 1175–1178.

–»– and S.-I. AKASOFU, 1975: The auroral electrojet and global auroral features. *J. Geophys. Res.* **80**, 3585–3602.

–»– and W. BAUMJOHANN, 1985: Estimation of electric fields and currents from IMS magnetometer data for the CDAW 6 intervals: Implications for substorm dynamics. *Ibid.,* **90**, 1305–1317.

KAMIDE, Y. and A. BREKKE, 1977: Altitude of the eastward and westward auroral electrojets. *Ibid.*, **82**, 2851–2853.

–»– and S. MATSUSHITA, 1979: Simulation studies of ionospheric electric fields and currents in relation to field-aligned current, 2. Substorm. *Ibid.*, **84**, 4099–4115.

–»– and J.E. VICKREY, 1983: Relative contribution of ionospheric conductivity and electric field to the auroral electrojets. *Ibid.*, **88**, 7989–7996.

KISABETH, J.L. and G. ROSTOKER, 1974: The expansive phase of magnetospheric substorm. 1. Development of the auroral electrojets and auroral arc configuration during a substorm. *Ibid.*, 79, 972–984.

KÜPPERS, F., UNTIEDT, J., BAUMJOHANN, W., LANGE, K. and A.G. JONES, 1979: A two-dimensional magnetometer array for ground-based observations of auroral zone electric currents during the International Magnetospheric Study (IMS). *J. Geophys.* **46**, 429–450.

LOGINOV, G.A., VASILJEV, E.P. and A. GRAFE, 1978: Some results of the investigation of magnetic variations of the auroral electrojets concluded from observations of the geomagnetic meridian project (GMP). *Gerl. Beitr. Geophys.* **87**, 249–262.

MERSMANN, U., BAUMJOHANN, W., KÜPPERS, F. and K. LANGE, 1979: Analysis of an eastward electrojet by means of upward continuation of ground-based magnetometer data. *J. Geophys.* **45**, 281–298.

PELLINEN, R.J., BAUMJOHANN, W., HEIKKILA, W.J., SERGEEV, V.A., YAHNIN, A.G., MARKLUND, G. and A.O. MELNIKOV, 1982: Event study on pre substorm phases and their relation to the energy coupling between solar wind and magnetosphere. *Planet. Space Sci.* **30**, 371–388.

PYTTE, T., McPHERRON, R.L., HONES, E.W. and H.J. WEST, 1978: Multiple-satellite studies of magnetospheric substorms: Distinction between polar magnetic substorms and convection-driven negative bays. *J. Geophys. Res.* **83**, 663–679.

ROSTOKER, G., WINNINGHAM, I.D., KAWASAKI, K., BURROWS, J.R. and K.I. HUGHES, 1979: Energetic particle precipitation into the high-latitude ionosphere and the auroral electrojets. 2. Eastward electrojet and field-aligned current flow at the dusk meridian. *Ibid.*, **84**, 2006–2018.

SPRENGER, K. and A. GRAFE, 1984: Radio aurora observations at medium latitude over two solar cycles. *J. Atmos. Terr. Phys.* **46**, 673–684.

TSUNODA, R.T., PRESNELL, R.I. and T.A. POTEMRA, 1976: The spatial relationship between the evening radar aurora and field-aligned currents. *Ibid.*, **81**, 3791–3802.

USPENSKY, M.V., PELLINEN, R.J., BAUMJOHANN, W., STARKOV, G.V., NIELSEN, E., SOFKO, G. and K.U. KAILA, 1983: Spatial variations of ionospheric conductivity and radar auroral amplitude in the eastward electrojet region during pre-substorm conditions. *J. Geophys.* **52**, 40–48.

VESTINE, E.H. and S. CHAPMAN, 1938: The electric current-system of geomagnetic disturbance. *Terrestr. Magn.* **43**, 351–382.

VICKREY, J.F., VONDRAK, R.R. and S.I. MATTHEWS, 1982: Energy deposition by precipitating particles and Joule dissipation in the auroral ionosphere. *J. Geophys. Res.* **87**, 5184–5196.

WALLIS, D.D., ANGER, C.D. and G. ROSTOKER, 1976: The spatial relationship of auroral electrojets and visible aurora in the evening sector. *Ibid.*, **81**, 2857–2869.

Appendix 1

Method for determination of the electrojet parameters

For the auroral electrojet flowing as a horizontal surface current in the ionosphere, certain parameters, like the width of the current layer, the current density, the total current intensity and the position of the electrojet centre, can be determined from the components of the geomagnetic variation field under certain assumptions. Methods for determination of the parameters have been presented by CHAPMAN (1951), WALKER (1964), SCRASE (1967), LANGEL and CAIN (1967) and CZECHOWSKY (1971).

A current layer which has a symmetric current density distribution around its centre is characterized by a disappearing vertical intensity ($\Delta Z = 0$) along the central line under the current layer. Therefore, the position of the electrojet centre is often being identifies as the position of the zero passage of the meridional ΔZ profile. This is the first assumption. Secondly, it is supposed that the auroral electrojets are flowing at a height of 100 to 120 km. This assumption is justified since it is obvious that these currents are flowing in the E layer, which also has been confirmed by direct rocket measurements (*e.g.*, REIMER 1969, POTTER 1970).

The third assumption which, is far more critical, deals with the meridional current density profile. In the past, model calculations have been carried out using the following current density profiles: constant current density (WALKER 1964), parabolically distributed current density (CHAPMAN 1951), Gauss-distributed current density and linearly from the centre decreasing current density (CZECHOWSKY 1971).

The components of the magnetic field are described by rather complicated expressions if one of the three last-named current density profiles is assumed. Therefore we decided to utilize for our calculations a profile of constant current density. Our method gives only the current density value averaged over the width of the profile. For a current layer of constant current density (i) the magnetic horizontal and vertical components according to the Biot-Savart law are as follows (neglecting the inductive part generated in the Earth's crust):

$$\Delta H = 2i \operatorname{arctg}\left(\frac{2ch}{h^2 + l^2 - c^2}\right) \tag{1}$$

$$\Delta Z = i \ln\left(\frac{(l+c)^2 + h^2}{(l-c)^2 + h^2}\right) \tag{2}$$

Where c = electrojet halfwidth, h = height of the electrojet and l = horizontal distance of the observation point to the centre of the layer. In these relations, only h is known by assumption. For the eastward electrojet, h = 120 km may be assumed. Knowing the value l from the observed ΔZ profile ($\Delta Z = 0$), c can be calculated if i is eliminated by the ratio $\Delta H/\Delta Z$. Then,

$$\frac{\Delta H}{\Delta Z} = \frac{2 \operatorname{arctg}\left(\frac{2ch}{h^2 + l^2 - c^2}\right)}{\ln\left(\frac{(l+c)^2 + h^2}{(l-c)^2 + h^2}\right)} \tag{3}$$

Since the direct calculation of c from $\Delta H/\Delta Z$ is very tedious, a graphical method is preferred. At first, curves $\Delta H/\Delta Z$ (l) are drawn for several values of c. These are represented in Fig. A1. They are characterized by a hyperbolic-like shape at which the radius of the drawn circle corresponds to the big semiaxis. This value (a) is depending on the width of the electrojet as shown in Fig. A2. By comparing the observed $\Delta H/\Delta Z$ profile curves with the model curves, c can easily be determined. It has to be taken into account that the scales in the model calculation and the observations are the same ones. The absolute accuracy is about ±40 km.

The procedure is the following: From the observed ΔH and ΔZ values along the magnetometer chain, meridional ΔH and ΔZ profiles are drawn. The ΔZ profile supplies the electrojet centre (at $\Delta Z = 0$) and thus the values l for each point in the profile. From these profiles, the most probable ($\Delta H/\Delta Z$) values are taken which then supply a sufficiently dense profile ($\Delta H/\Delta Z$) that is necessary for an exact determination of c. After derivation of the width of the current layer the current density is obtained from the intensity of the horizontal disturbance vector in the centre of the current layer. From (1), then follows ($l = 0$)

$$i = \frac{1}{2} \frac{\Delta H}{\operatorname{arc\,tg}\left(\frac{2ch}{h^2 - c^2}\right)} \tag{4}$$

According to CHAPMAN (1919) and AKASOFU (1960) only about 60 % of the observed horizontal component is given by the external induced field, which has been considered in the calculation of the current density. The total current I of the current layer is calculated according to the relation:

$$I = 2ci \tag{5}$$

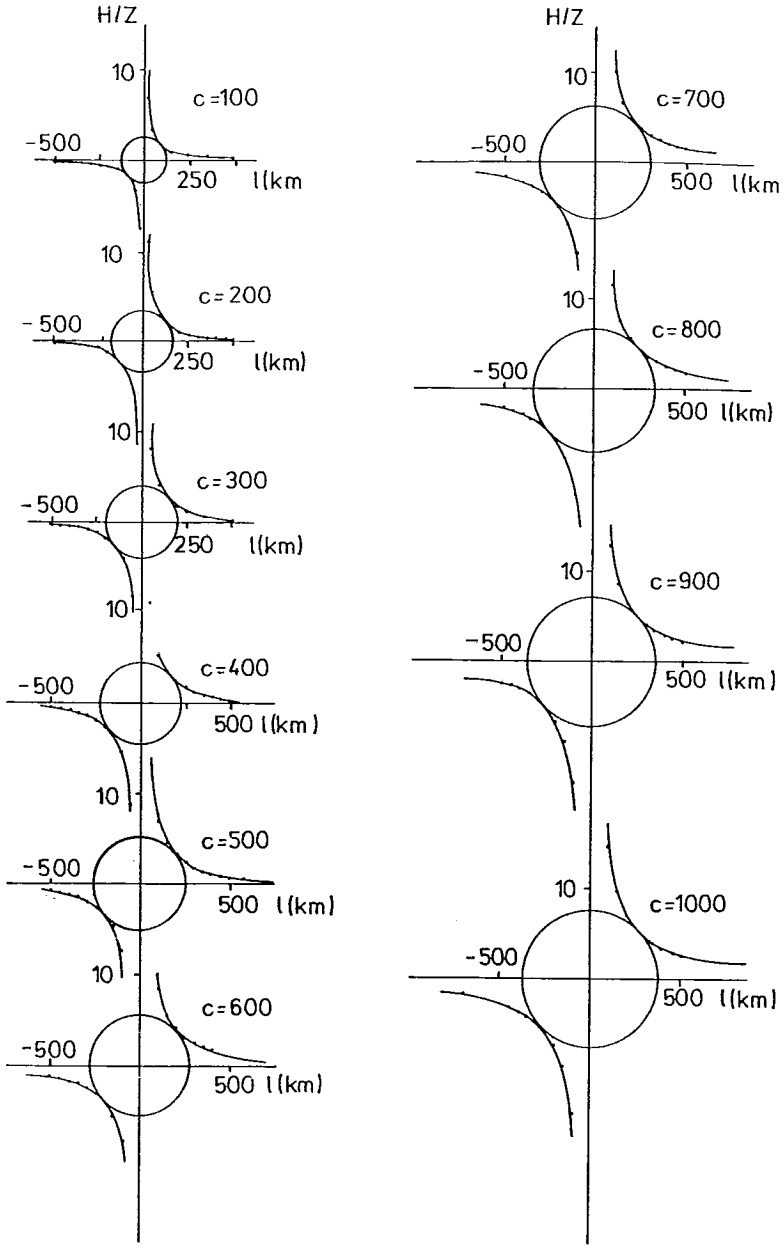

Fig. A1. Modelcurves for the relationship between H/Z and 1 (km). Radius of the circle is the model parameter used in Fig. 2.

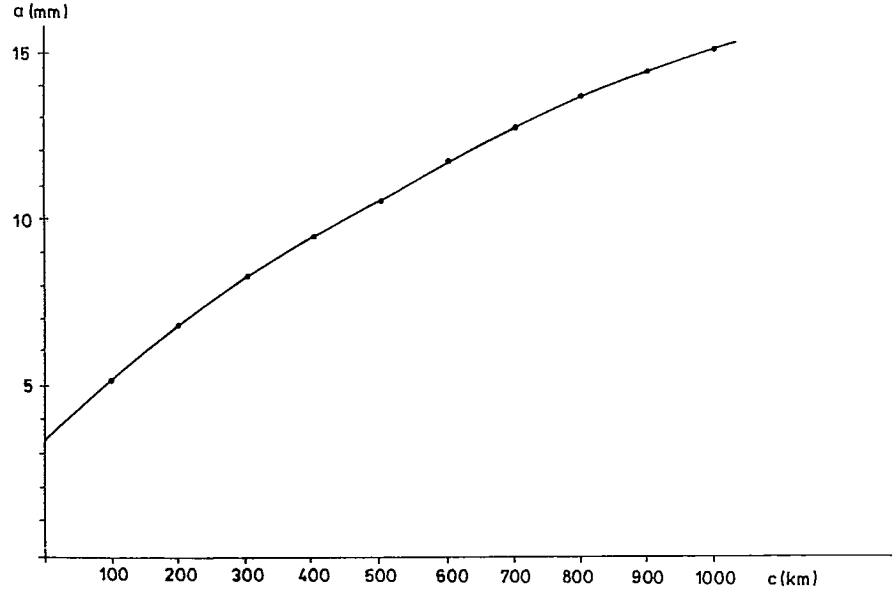

Fig. A2. Dependence of parameter a on electrojet half-width c. This is valid for H/Z-axis: 10 $\hat{=}$ 2 cm and 1-axis: 1000 km $\hat{=}$ 4 cm.